ELSEVIER

Chemical Engineering Journal 128 (2007) 11–20

Chemical Engineering Journal

www.elsevier.com/locate/cej

Influence of ionic strength on complex formation between poly(ethylene oxide) and cationic surfactant and turbulent wall shear stress in aqueous solution

Siriluck Suksamranchit, Anuvat Sirivat *

The Petroleum and Petrochemical College, Chulalongkorn University, Bangkok 10330, Thailand

Received 8 March 2006; received in revised form 22 August 2006; accepted 3 October 2006

Abstract

We investigate the influence of ionic strength on the interaction between poly(ethylene oxide) (PEO) and cationic surfactant, hexadecyltrimethylammonium chloride (HTAC), and the consequent effect on turbulent drag reduction in aqueous PEO/HTAC solutions. Conductivity and surface tension data for PEO-HTAC in aqueous solution indicate that salt stabilizes binding of HTAC micelles to the polymer. Dynamic light scattering analysis indicates an increase in hydrodynamic radius for HTAC micelles in aqueous salt solution. In contrast, salt reduces the hydrodynamic radius of PEO-HTAC complexes. The latter observation is consistent with contraction of the PEO-HTAC complex via electrostatic screening. For the measurement of turbulent drag reduction in a Couette cell, our data indicate that the minimum wall shear stress in aqueous HTAC solutions occurs at an optimum HTAC concentration, close to CMC, and this optimum concentration value decreases with increasing ionic strength. This result suggests a lowering of the CMC in turbulent flow. For aqueous PEO-HTAC mixtures, the minimum wall shear stress occurs at an optimum PEO concentration smaller than that of pure PEO solutions, and this optimum concentration value increases with ionic strength. Our findings provide evidences that the turbulent wall shear stress does not always scale inversely with the hydrodynamic volume of the polymer–surfactant complex.

Keywords: Turbulent drag reduction; Poly(ethylene oxide); Cationic surfactant; Hexadecyltrimethylammonium chloride; Ionic strength

1. Introduction

The addition of small amounts of high-molecular weight polymers or surfactants to a fluid in a fully developed turbulent flow can cause a dramatic reduction of the turbulent wall shear stress [1–3]. This phenomenon, known as turbulent drag reduction (DR), was discovered more than fifty years ago [4]. Numerous applications of DR are known, including transportation of crude oil in oil pipelines, increased jet velocity and beam focusing in fire fighting equipment, prevention of over dosage of water flow during heavy rain in drainage and irrigation systems, increase of volumetric flow rate of fluid in hydro-power systems, and improvement of blood flow in partially blocked arteries in biomedical studies [5–9].

The mechanism of turbulent drag reduction has been explored extensively since the original discovery by Toms [4], who, prompted by Oldroyd's theory of wall slip [10], first proposed the idea that the polymer creates a shear thinning layer at the wall having an extremely low viscosity. Subsequently, Lumley [11–13] suggested that there is a critical value of wall shear stress, at which macromolecules become stretched due to the fluctuating strain rate. However, in the viscous sublayer close to the wall, polymer coils are not greatly deformed and viscosity does not increase greatly above that of the solvent alone. In the turbulent zone, the macromolecular extension yields a dramatic increase in viscosity, which damps small dissipative eddies, and reduces momentum transport towards the viscous sublayer, resulting in a thickening of the sublayer and a reduction of the drag. Virk [14] suggested that, at the onset of turbulent drag reduction, the duration of a turbulent burst is of the order of the terminal relaxation time of a macromolecule, and proposed that energy dissipation via macromolecular extension is involved in the mechanism of drag reduction. Hlavacek et al. [15] proposed that, in turbulent flow, the solvent contains microdisturbances or turbulence precursors. Macromolecules suppress turbulence by pervading two or more of these microdomains

* Corresponding author. Tel.: +662 218 4131; fax: +662 611 7221.
E-mail address: anuvat.s@chula.ac.th (A. Sirivat).

1385-8947/$ – see front matter © 2006 Elsevier B.V. All rights reserved.
doi:10.1016/j.cej.2006.10.003

simultaneously and hindering their free movement and growth. De Gennes [16,17] developed a model based on the Kolmogorov energy cascade theory, and considering the ability of polymer molecules to store the elastic energy upon deformation. When this elastic energy is comparable to the kinetic energy of a particular turbulent eddy, the energy cascade is suppressed. Ryskin [18] proposed the yo-yo model, as the mechanism by which polymer molecules unravel in an extensional flow field associated with turbulence. The central portion of the chain straightens, while the end portions remain coiled. When the flow becomes weak, the polymer chain retracts into a fully-coiled state. The taut central portion generates a large stress and facilitates viscous dissipation of turbulent kinetic energy.

Polymers and surfactants have received considerable attention among available drag reducing additives [19,20]. In general, effective drag reducing polymers should possess a linear flexible structure and a very high molecular weight [19]. One polymer known to be suitable for use as a drag reducer is poly(ethylene oxide) (PEO) [21]. This polymer is commercially available over a wide range of molecular weights. Previous studies [19,22] report that drag reduction for PEO solutions is observed above a critical molecular weight, M_c (for the double Couette geometry used in our experiments [22], $0.91 \times 10^5 < M_c < 3.04 \times 10^5$ g/mol). Maximum drag reduction occurs at an optimum concentration, c^*_{PEO}, which scales inversely with molecular weight, and the percent maximum drag reduction increases with molecular weight [19,22]. However, polymers are susceptible to high shear degradation, and are therefore limited to a single throughput application. Certain surfactants form large wormlike or network microstructures in solution which are thermodynamically stable and self-assemble quickly after degradation, restoring drag reducing power. For this reason, there have become of increasing interest as drag reducing additives recently. Among the drag reducing surfactants, the cationic species (hexadecyltrimethylammonium chloride, HTAC) has been shown to be an effective drag reducer [23,24], when used in combination with organic counterions, which facilitate the formation of wormlike micellar structures.

Recent studies have demonstrated that water-soluble polymers like PEO form complexes with cationic surfactants such as HTAC [25–28] in which surfactant micelles are bound to the polymer. The formation of such complexes causes characteristic changes in solution viscosity, because of the increased hydrodynamic volume of the complex. In a previous study [22], we investigated the effect of complex formation between PEO and HTAC on the drag reduction behavior of PEO solutions, and showed that the critical PEO molecular weight for drag reduction decreases, interpreted as due to the increase in hydrodynamic volume when HTAC micelles bind to PEO. Also, consistent with this interpretation, at fixed PEO concentration, maximum drag reduction is observed at an optimum HTAC concentration, $c^*_{HTAC\text{-}PEO}$, comparable to the maximum binding concentration (MBC), where polymer chains are saturated with surfactants [22]. Moreover, with HTAC concentration fixed at the MBC, the optimum PEO concentration for drag reduction, $c^*_{PEO\text{-}HTAC}$, decreases relative to that, c^*_{PEO}, in the absence of HTAC [22].

Addition of salt stabilizes the binding of HTAC micelles to the PEO due to the screening of electrostatic repulsions between the surfactant head groups [28]. The number of PEO chains incorporated into PEO-HTAC complexes in aqueous salt solution is smaller than that in the salt-free PEO-HTAC complex [28], i.e. dissociation of multichain complexes occurs in the polymer–surfactant complex solutions when salt is added [28]. These observations motivate the present study, first, to investigate the effect of ionic strength on the hydrodynamic radius of pure surfactant in solution and compare the results with those for the polymer–surfactant complex. Second, we study the consequent effect of these changes in structure on turbulent drag reduction. Based on these observations, we discuss whether polymer–surfactant complex formation survives under turbulent flow conditions, and hence produces a synergistic response in the drag reduction characteristics of PEO and HTAC in aqueous salt solution.

2. Experimental

2.1. Materials and sample preparation

Poly(ethylene oxide) of quoted molecular weights 6.00×10^5 and 40.0×10^5 g/mol, designated PEO6 and PEO20 were purchased from Aldrich Chemical Co. and used without further purification. The cationic surfactant was hexadecyltrimethylammonium chloride ($C_{16}H_{33}N(CH_3)_3Cl$), a commercial product donated by Unilever Holding Inc., used as received. The surfactant solution contains 50% HTAC, 36% H_2O and 14% isopropanol. Analytical grade sodium chloride (NaCl), at 99.5% minimum assay (Carlo Erba Reagenti Co.) was used to vary ionic strength of the complex solutions. Distilled water was used as a solvent after two times filtration through 0.22 μm Millipore membrane filters to remove dust particles. The polymer stock solutions were prepared as w/v (%) in distilled water at room temperature by dissolving PEO in distilled water and by gentle stirring for a period of 4–10 days, depending on polymer concentration and molecular weights. Surfactant and polymer–surfactant complex solutions were prepared by adding appropriate amounts of HTAC and NaCl into mixtures of distilled water and polymer stock solutions and by gentle stirring for 24 h at room temperature. Before light scattering measurements, the polymer–surfactant complex solutions were centrifuged at 10,000 rpm for 15 min and then filtered directly into the light scattering cell through 0.45 μm Millipore membranes. All measurements were carried out at a temperature of 30 °C.

2.2. Procedures

Static and dynamic light scattering (SLS and DLS) measurements (Malvern Instruments Company, model 4700) were carried out at 30 °C. The light source was an argon laser emitting vertically polarized light at wavelength 514.5 nm. DLS was used to determine the apparent diffusion coefficient, $\langle D_{app} \rangle$, at different scattering angles θ, and the center of mass diffusion coefficient, D_{cm}, was obtained by linear extrapolation of $\langle D_{app} \rangle$

to zero scattering angle:

$$\langle D_{\text{app}} \rangle = D_{\text{cm}} (1 + Cq^2 R_{\text{g}}^2 + \cdots) \quad (1)$$

where C is a coefficient influenced by the slowest internal mode of motion of the particle and by the size, flexibility and polydispersity of the polymer [29]. R_{g} is the radius of gyration of the polymer chain. q is the scattering wave vector. The diffusion coefficient at infinite dilution, D_0, is obtained by linear extrapolation of D_{cm} to zero concentration, c_{s}:

$$D_{\text{cm}} = D_0(1 + k_{\text{D}} c_{\text{s}} + \cdots) \quad (2)$$

where k_{D} (l/g) describes the concentration dependence of D_{cm} (m^2/s) due to thermodynamic and hydrodynamic interactions. The hydrodynamic radius is calculated from D_0 (m^2/s) using the Stokes–Einstein equation:

$$R_{\text{h}} = \frac{k_{\text{B}} T}{6\pi\eta_{\text{s}} D_0} \quad (3)$$

where k_{B} is Boltzmann's constant (N m/K), T the absolute temperature (K) and η_{s} is the viscosity of solvent (kg/m s). This equation is based on the assumption of spherical aggregates with uniform shape and size. In this study, DLS was performed to determine the hydrodynamic radius of surfactant micelles and PEO-HTAC complexes at 30 °C.

Static light scattering (SLS) was used to determine the weight-average molecular weight, M_{w}, of PEO samples via the Zimm-Debye equation [30]. In the small-angle limit, this can be expressed as

$$\frac{Kc}{\Delta R_\theta} = \frac{1}{M_{\text{w}}} \left(1 + \frac{(q^2 R_{\text{g}}^2)}{3} \right) + 2A_2 c \quad (4)$$

where M_{w} is the weight-average molecular weight, A_2 the second osmotic virial coefficient, R_{g}^2 the z-average of the mean square radius of gyration, ΔR_θ indicates the excess Rayleigh ratio:

$$\Delta R_\theta = \frac{\Delta I_{\theta(\text{solution})}}{I_{\theta(\text{standard})}} \times R_{\theta(\text{standard})} \times \frac{n^2_{(\text{solution})}}{n^2_{(\text{standard})}} \quad (5)$$

Here, $\Delta I_{\theta(\text{solution})}$ is the excess scattered intensity of the sample solution relative to the solvent, $n_{(\text{solution})}$ and $n_{(\text{standard})}$ the refractive indices of the sample solution and reference fluid and K is the optical constant:

$$K = \frac{4\pi^2 n^2 (\text{d}n/\text{d}c)^2}{N_{\text{A}} \lambda^4} \quad (6)$$

where n is the refractive index of the solvent, c the polymer concentration (g/cm^3), λ the wavelength of incident light (514.5 nm), dn/dc the refractive index increment (cm^3/g), N_{A} the Avogadro's number and q is the scattering wave vector (cm^{-2}). Toluene (AR grade, Lab-Scan) was used as a reference fluid, having a Rayleigh ratio at 514.5 nm of 3.2×10^{-5} cm^{-1}. M_{w} of PEO6 and PEO20 were determined by SLS to be 6.06×10^5 and 17.9×10^5 g/mol, respectively.

A conductivity meter (Orion Co., model 160) was used to characterize the electrical conductivity of polymer and surfactant complex solutions in the absence and presence of NaCl.

The equilibrium surface tension of polymer and surfactant complex solutions was measured by a pendant drop tensiometer (Kruss, model DSA10-Mk2). The shape of the sample drop was analyzed automatically and converted to surface tension.

Wall shear stress measurements, τ_{w}, were carried out using a fluids rheometer (Rheometrics, ARES), equipped with two Couette cells: a single Couette cell (SCU), and a double Couette cell (DCU). The single Couette cell has a cup radius of 23.95 mm and a bob radius of 20.0 mm. For the double Couette cell, the radii of the outer cup and the outer bob are identical to those of the single Couette cell, while the inner cup and inner bob radii are $R_{\text{IC}} = 7.2$ mm and $R_{\text{IB}} = 18.05$ mm, respectively. The bob length, L, is 40.0 mm and the vertical gap between the upper bob and the lower cup was set at 0.05 mm. From these parameters, we calculated the aspect ratio, $\alpha = L/(R_{\text{IB}} - R_{\text{IC}})$ and the radius ratio, $\eta = R_{\text{IC}}/R_{\text{IB}}$, of our Couette cell to be 3.69 and 0.40, respectively. The small value of η indicates that our experiment was carried out under the wide gap condition. The temperature was controlled by a water bath controller at 30.0 ± 1.0 °C. The single Couette cell generates a laminar flow whereas the double Couette cell was designed to generate identical laminar flow between the outer cup and bob, and turbulent flow between the inner cup and bob. The torque was measured by a transducer connected to the upper bob. The inner wall shear stress, τ_{w} (N/m^2), of the sample was computed as the difference between the total torque measured by the DCU and the torque measured by the SCU according to the following equation:

$$\tau_{\text{w}} = (M_{\text{DCU}} - M_{\text{SCU}}) K_\tau \quad (7)$$

where M_{DCU} (N m) is the total DCU torque, M_{SCU} the SCU torque and K_τ (m^{-3}) is a stress constant, which can be expressed as

$$K_\tau = \tfrac{1}{2}\pi L (R_{\text{IB}})^2 \quad (8)$$

where L is the bob length (m) and R_{IB} is the inner radius of the bob (m). The inner shear strain rate was calculated from the relation

$$\gamma = \theta K_\gamma \quad (9)$$

where γ is shear rate (s^{-1}), θ the angular velocity (s^{-1}) and K_γ is a strain constant which can be expressed as

$$K_\gamma = \frac{2}{1 - (R_{\text{IC}}/R_{\text{IB}})^2} \quad (10)$$

The Reynolds number (Re) can be calculated for the inner chamber of the double Couette cell using the following equation

$$Re = \frac{\theta R_{\text{IC}} (R_{\text{IB}} - R_{\text{IC}})}{\nu} \quad (11)$$

where ν is the kinematic viscosity of sample solutions (m^2/s).

For the Couette cells used in this experiment, the critical Reynolds number, Re_{c} for the laminar to turbulent transition is $Re_{\text{c}} \cong 1000$. Above this critical Reynolds number, a turbulent flow is generated. Our result is consistent with the previous work carried out by Sparrow et al. [35]. They investigated the onset

of turbulence transition in a wide gap Couette cell and found $Re_c \cong 1600$.

During the wall shear stress measurement of polymer and surfactant aqueous solutions in turbulent flow especially using high M_w polymer, the molecular degradation of polymer during test cannot be totally avoided. In our experiment, we minimized polymer degradation by using only fresh samples and the initial DR efficiency was investigated and reported. The duration of each experiment was kept short about 10 min. In some experiments, we remeasured the torque versus shear rate relations a few times; they differed by few percents and lie within experimental error bars. We may assume that mechanical degradation, if present, was not significant to affect our data.

To avoid foam formation during sample preparation, we gently poured down the sample into the Couette cell and then adjusted the measuring temperature to be 30 °C and waited for a period of 5 min before each DR measurement. This waiting period allows the gravity force to act on the liquid lamellae between air bubbles and thus reducing existing foams. During the DR measurements, there could possibly be foam formation, but we did not or could not observe visually. We note that a cationic surfactant has lower foam formation ability than anionic surfactant (CMC of a cationic surfactant is higher). Low surfactant concentrations were used in our experiment (maximum HTAC concentration used in our experiment is 5 mM which is about four times of CMC), and since the sample solutions have very low viscosity foams can be easily destroyed by gravity force.

3. Results and discussions

The physicochemical properties of aqueous solutions of surfactant–polymer complexes were investigated at 30 °C. As noted in Table 1, two specimens were utilized, PEO6 and PEO20, whose weight-average molecular weights, M_w, were determined from SLS measurement to be 6.06×10^5 and 17.9×10^5 g/mol, respectively. The measured M_w for PEO6 is quite close to the manufacturer quoted value, whereas, for PEO20, the measured M_w is substantially smaller. This suggests that the high-end portion of the molecular weight distribution was removed during filtration of solutions prior to experimental measurements. Previous studies [22] showed that the optimum PEO concentrations, c^*_{PEO}, for maximum drag reduction in pure PEO solutions, measured as the minimum value of τ_w in the double Couette rheometer via Eq. (7) are 40 ppm (0.91 mM/PEO repeating unit) and 15 ppm (0.34 mM/PEO repeating unit) for specimens PEO6 and PEO20, respectively. Here, the maximum %DR is 68% for 40 ppm of PEO6 and 85% for 15 ppm of PEO20. Table 1 lists values of the critical aggregate concentration (CAC), corresponding to the onset of surfactant binding to the polymer, the critical micelle concentration (CMC), at which free micelles form in the surfactant–polymer solution, and the maximum binding concentration (MBC), the surfactant concentration at which the PEO becomes saturated with bound surfactant. The CAC, CMC and MBC were determined, as described below, from measurements of conductivity and surface tension of PEO-HTAC complexes in aqueous NaCl solutions, whose PEO concentrations were fixed at the respective values, c^*_{PEO}, where the maximum drag reduction of PEO solutions is observed in the absence of surfactant.

3.1. Critical aggregate concentration, critical micelle concentration and maximum binding concentration

The CAC and CMC were determined at 30 °C by two methods: conductivity and surface tension; the MBC was determined from surface tension measurements. Figs. 1–3 show conductivity as a function of HTAC concentration for aqueous solutions of HTAC and HTAC-NaCl (Fig. 1), PEO6-HTAC, and PEO6-HTAC-NaCl mixtures (Fig. 2), and PEO20-HTAC, and PEO20-HTAC-NaCl mixtures (Fig. 3). The PEO6 concentration was fixed at $c^*_{PEO} = 40$ ppm while the PEO20 concentration was set at $c^*_{PEO} = 15$ ppm; in each case, two different values of mole ratio were investigated, [NaCl]/HTAC] = 1/1 and 5/1. In Fig. 1a–c, the first and only transition in slope of a plot of conductivity versus HTAC concentration identifies the CMC for HTAC and HTAC-NaCl solutions. In Figs. 2 and 3, the CAC is

Table 1
Conductivity and surface tension data of PEO-HTAC-NaCl complexes in quiescent aqueous solution at 30 °C

Codes of system studied	PEO M_w (g/mol)	c^*_{PEO} [a] (ppm)	Conductivity		Surface tension[b]		
			CAC[c] (mM)	CMC[d] (mM)	CAC (mM)	CMC (mM)	MBC[e] (mM)
HTAC	–	–	–	1.30	–	1.30	–
[NaCl]/[HTAC] = 1/1	–	–	–	0.70	–	N/A	–
[NaCl]/[HTAC] = 5/1	–	–	–	0.60	–	N/A	–
PEO6_40 + HTAC	6.06×10^5	40	0.19	1.65	0.16	1.70	0.25
PEO6_40 + [NaCl]/[HTAC] = 1/1	6.06×10^5	40	N/A	1.20	0.13	1.20	0.27
PEO6_40 + [NaCl]/[HTAC] = 5/1	6.06×10^5	40	N/A	1.00	0.13	1.15	0.35
PEO20_15 + HTAC	17.9×10^5	15	0.19	1.80	0.18	1.80	0.20
PEO20_15 + [NaCl]/[HTAC] = 1/1	17.9×10^5	15	N/A	1.50	0.10	1.50	0.30
PEO20_15 + [NaCl]/[HTAC] = 5/1	17.9×10^5	15	N/A	1.00	0.10	1.00	0.40

[a] c^*_{PEO} is the optimum PEO concentration in which maximum drag reduction is obtained.
[b] The uncertainties of data determined from surface tension measurement are ±10%.
[c] CAC is the critical aggregate concentration: concentration in which surfactant molecules start to interact with polymer.
[d] CMC is the critical micelle concentration: concentration in which free surfactant micells start to form.
[e] MBC is the maximum binding concentration: surfactant concentration in which a polymer chain contains a maximum number of surfactant molecules.

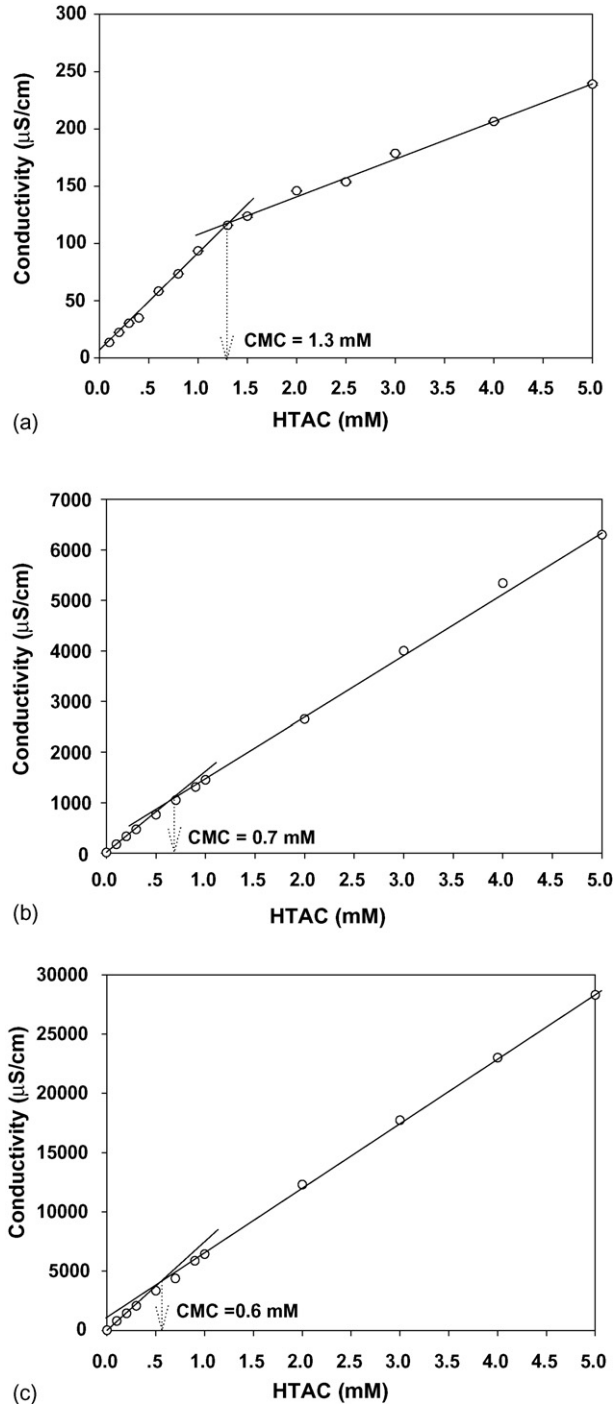

Fig. 1. Variation of the conductivity with surfactant concentration at 30 °C for aqueous solutions of: (a) pure HTAC; (b) [NaCl]/[HTAC] = 1/1, the mole ratio of NaCl to HTAC equal to 1; and (c) [NaCl]/[HTAC] = 5/1, the mole ratio of NaCl to HTAC equal to 5.

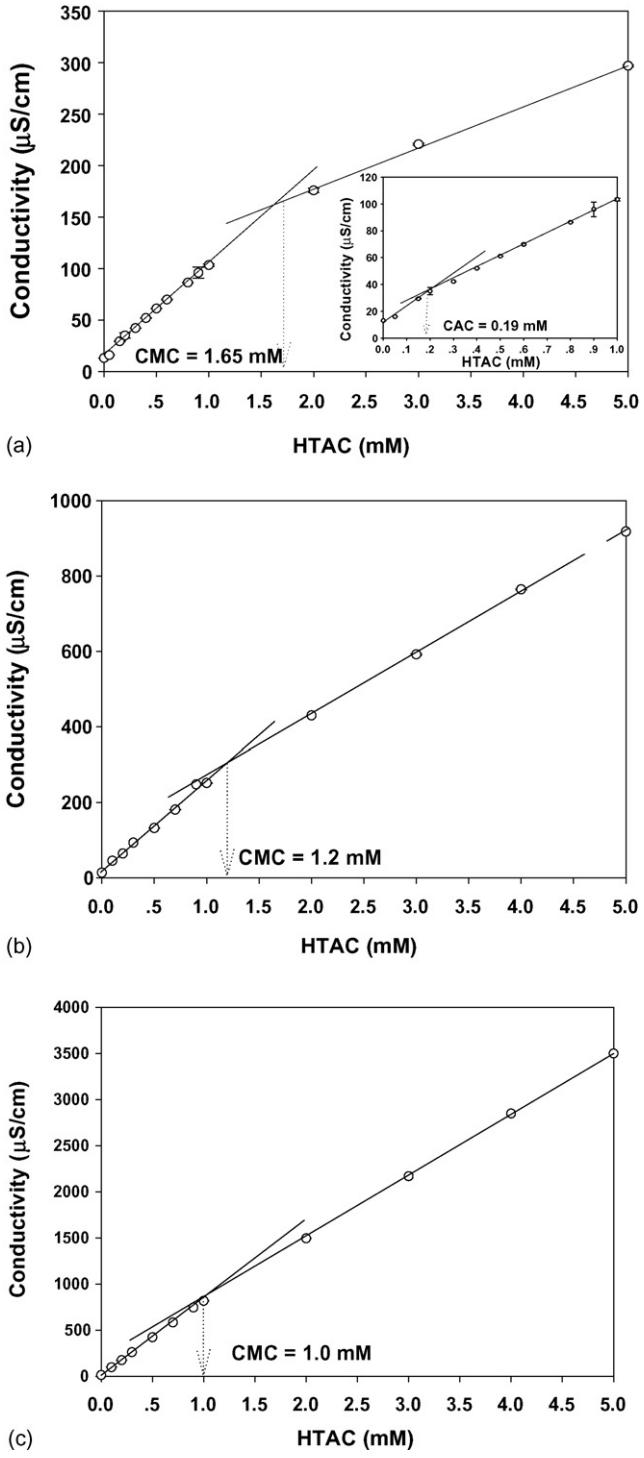

Fig. 2. Variation of the conductivity with surfactant concentration at 30 °C for aqueous solutions of: (a) PEO6_40 + HTAC, PEO M_w 6.06×10^5 g/mol, 40 ppm; (b) PEO6_40 + [NaCl]/[HTAC] = 1/1, PEO $M_w = 6.06 \times 10^5$ g/mol, 40 ppm, and the mole ratio of NaCl to HTAC equal to 1; and (c) PEO6_40 + [NaCl]/[HTAC] = 5/1, PEO $M_w = 6.06 \times 10^5$ g/mol, 40 ppm, and the mole ratio of NaCl to HTAC equal to 5.

identified as the initial change in slope, and the CMC as the second slope change. However, the CAC is clearly discernable only in the absence of salt (Figs. 2a and 3a), and therefore surface tension measurements had to be used instead. The corresponding CAC and CMC values are listed in Table 1.

Fig. 4 exhibits the variation of surface tension with HTAC concentration for PEO6-HTAC solutions having PEO6 at 40 ppm, without salt, and with salt added at mole ratios [NaCl]/[HTAC] of 1.0 and 5.0. As evident in Fig. 4, the surface tension decreases on addition of HTAC, and the CAC values is located as the initial HTAC concentration at which a discrete

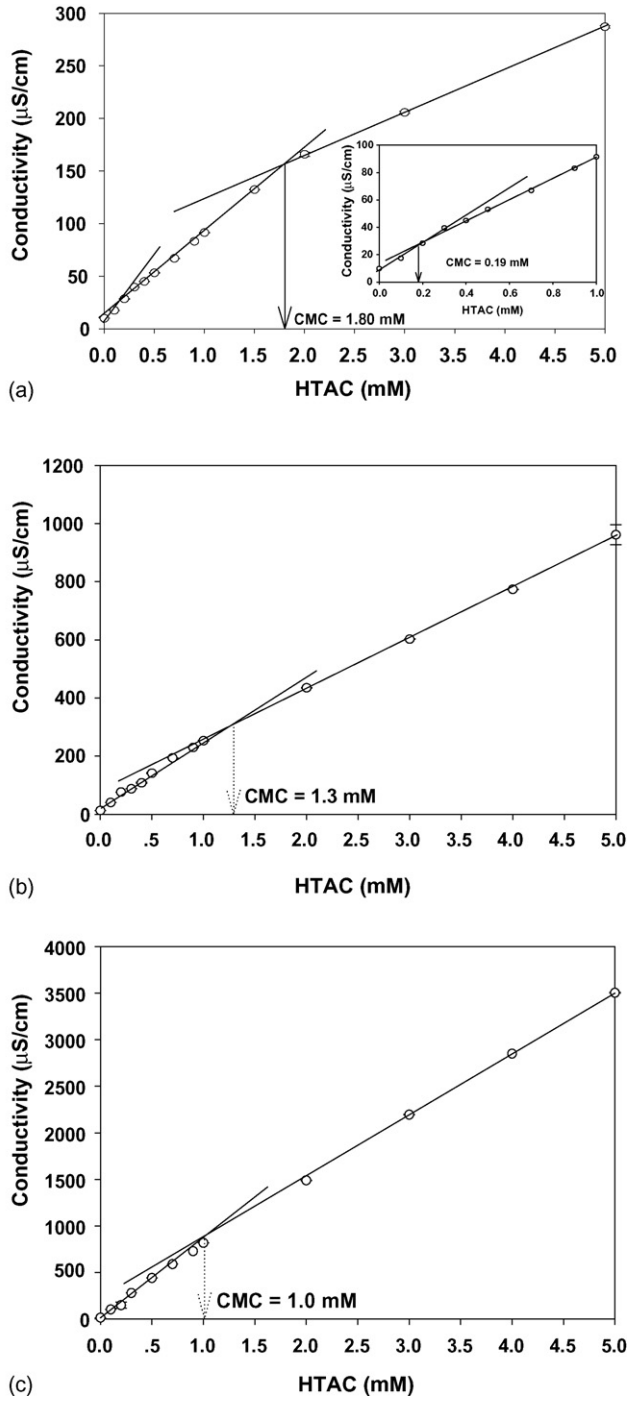

Fig. 3. Variation of the conductivity with surfactant concentration at 30 °C for aqueous solutions of: (a) PEO20_15 + HTAC, PEO $M_w = 17.9 \times 10^5$ g/mol 15 ppm; (b) PEO20_15 + [NaCl]/[HTAC] = 1/1, PEO $M_w = 17.9 \times 10^5$ g/mol, 15 ppm, and the mole ratio of NaCl to HTAC equal to 1; and (c) PEO20_15 + [NaCl]/[HTAC] = 5/1, PEO $M_w = 17.9 \times 10^5$ g/mol, 15 ppm, and the mole ratio of NaCl to HTAC equal to 5.

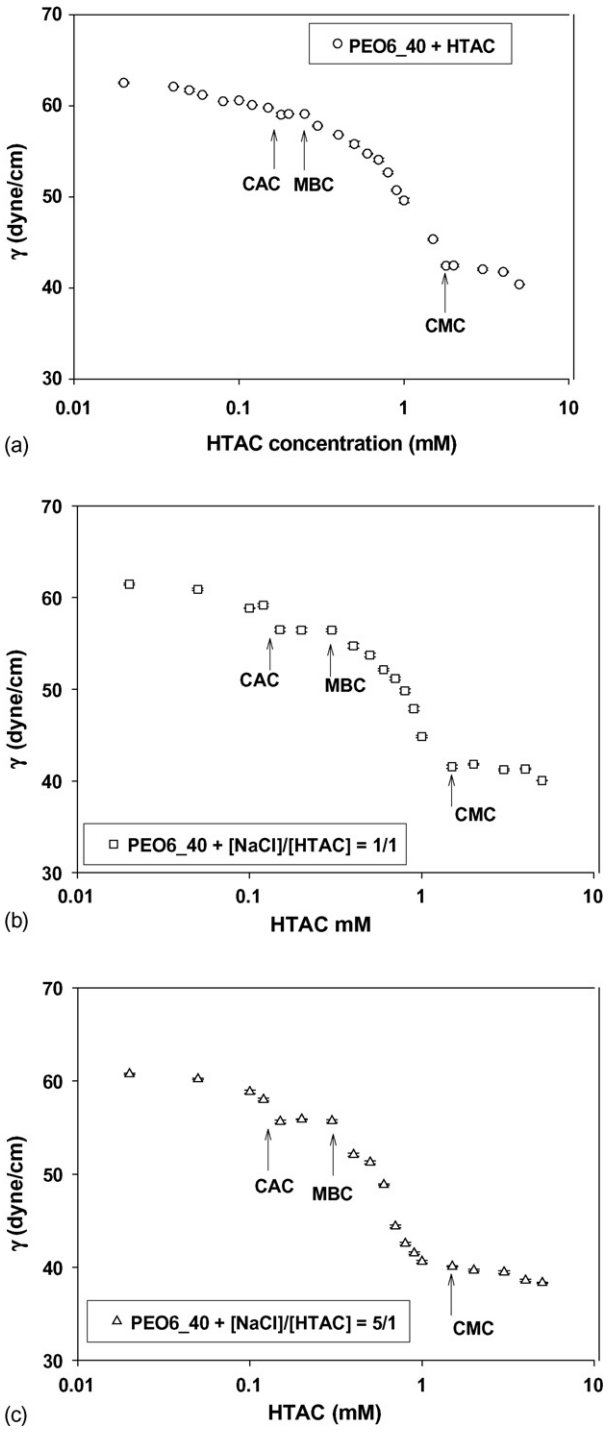

Fig. 4. Variation of the surface tension with surfactant concentration at 30 °C for aqueous solutions of: (a) PEO6_40 + HTAC, PEO $M_w = 6.06 \times 10^5$ g/mol at 40 ppm; (b) PEO6_40 + [NaCl]/[HTAC] = 1/1, PEO $M_w = 6.06 \times 10^5$ g/mol, 40 ppm, and the mole ratio of NaCl to HTAC equal to 1; and (c) PEO6_40 + [NaCl]/[HTAC] = 5/1, PEO $M_w = 6.06 \times 10^5$ g/mol, 40 ppm, and the mole ratio of NaCl to HTAC equal to 5.

change to a regime of constant surface tension occurs. Subsequently, the surface tension begins to decrease again, and this point is identified as the MBC, i.e. where the PEO chains have become saturated with bound HTAC. Finally a third transition point occurs where the surface tension levels off and no further decrease occurs with addition of HTAC. This corresponds to the CMC. These characteristic transitions are indicated by arrows in Fig. 4, and the corresponding CAC, MBC and CMC values are listed in Table 1.

From Table 1, we see that the CAC and CMC values for PEO-HTAC complexes in aqueous solution from surface ten-

Table 2
Dynamic light scattering data of PEO-HTAC-NaCl complexes quiescent in aqueous solutions at 30 °C

Codes of system studied	c^*_{PEO} (ppm)	c^*_{PEO} (mM of PEO repeating unit)	$D_0 \times 10^{12}$ (m^2/s)	R_h (nm)	$\mu_2/\bar{\Gamma}^2$
HTAC 1.3 mM[a]	–	–	170 ± 2.00	1.31 ± 0.015	0.16
HTAC 0.7 mM + [NaCl]/[HTAC] = 1/1[a]	–	–	99.8 ± 2.04	2.23 ± 0.045	0.17
HTAC 0.6 mM + [NaCl]/[HTAC] = 5/1[a]	–	–	90.7 ± 1.53	2.45 ± 0.041	0.07
PEO6_40 + HTAC 5 mM[b]	40	0.91	3.98 ± 0.20	55.9 ± 2.81	0.83
PEO6_40 + HTAC 5 mM + [NaCl]/[HTAC] = 1/1[b]	40	0.91	4.92 ± 0.03	45.1 ± 0.23	0.21
PEO6_40 + HTAC 5 mM + [NaCl]/[HTAC] = 5/1[b]	40	0.91	4.59 ± 0.03	48.4 ± 0.34	0.23
PEO20_15 + HTAC 5 mM[b]	15	0.34	2.40 ± 0.17	92.7 ± 6.73	0.61
PEO20_15 + HTAC 5 mM + [NaCl]/[HTAC] = 1/1[b]	15	0.34	3.08 ± 0.05	72.2 ± 1.21	0.25
PEO20_15 + HTAC 5 mM + [NaCl]/[HTAC] = 5/1[b]	15	0.34	2.90 ± 0.03	76.4 ± 0.81	0.22
PEO20_15 + HTAC 0.2 mM[c]	15	0.34	2.90 ± 0.10	76.5 ± 0.26	0.45
PEO20_15 + HTAC 0.2 mM + [NaCl]/[HTAC] = 1/1[c]	15	0.34	3.50 ± 0.06	63.3 ± 0.11	0.35
PEO20_15 + HTAC 0.2 mM + [NaCl]/[HTAC] = 5/1[c]	15	0.34	3.22 ± 0.06	68.9 ± 0.13	0.34

[a] HTAC concentration is fixed at CMC of each solution.
[b] HTAC concentration is fixed at maximum HTAC concentration for wall shear stress measurement.
[c] HTAC concentration is fixed at MBC of each solution.

sion are consistent with those obtained from conductivity. We also find that the CAC and CMC values in salt solution are lower than in water. Increase in ionic strength, promotes the formation of HTAC micelles and PEO-HTAC complexes due to a reduction in electrostatic repulsions between the ionic surfactant head groups which stabilizes the surfactant micelle structure, as shown previously [28]. We further find that, at a given NaCl/HTAC mole ratio, the CMC values of the PEO-HTAC solutions are higher than those of the pure surfactant. The increase of the CMC in PEO-HTAC complex solutions corresponds quantitatively to the amount of PEO-bound surfactant. Finally, from Table 1, we find that, as salt is added a higher MBC value is observed, which, combined with a decreasing trend in CAC, indicates an increase in the amount of surfactant molecules bound to the PEO chains, again reflective of an increase in PEO-HTAC complex stability due to the screening of electrostatic repulsions between surfactant head groups. Table 1 also contains results for solutions containing high-molecular weight PEO, i.e. PEO20 at 15 ppm without salt, and with added salt, having mole ratios [NaCl]/[HTAC] = 1/1 and 5/1. Uncertainties of the data obtained from surface tension measurement typically vary within 10%. However, it appears that there is no substantive change in surface tension values when comparing the solutions containing HTAC complexed to high versus low molecular weight (PEO20 at 15 ppm cf. PEO6 at 40 ppm). This result is consistent with the previous observation of Schwuger [30] who found that the surface tension of solutions of PEO, complexed with an anionic surfactant, SDS (PEO $M_w > 4000$) was independent of PEO molecular weight. The MBC values of PEO-HTAC solutions are tabulated in Table 1.

To summarize the above results, the addition of salt leads to a reduction of the CMC and CAC but an increase in MBC of PEO-HTAC solutions. These effects indicate, respectively, a reduction in electrostatic repulsions between the positive surfactant head groups of micelles and an increase in binding affinity between the surfactant and the PEO chain.

3.2. Dynamic light scattering measurements

Table 2 lists values of the diffusion coefficient, D_0, hydrodynamic radius, R_h and normalized second cumulant, $\mu_2/\bar{\Gamma}^2$, obtained from dynamic light scattering measurement of aqueous PEO-HTAC-NaCl complex solutions at 30 °C. Uncertainties indicate standard deviations obtained from repeated measurements on the same samples. For HTAC and NaCl-HTAC solutions, D_0, R_h and $\mu_2/\bar{\Gamma}^2$, were determined at the corresponding CMC. The micellar radii, R_h, in the absence of salt and with salt added at molar ratios [NaCl]/[HTAC] = 1/1 and 5/1 are, respectively, 1.31, 2.23 and 2.47 nm, indicating that, as expected, added salt increases the aggregation number and size of HTAC micelles. For PEO6 and PEO20 solutions, D_0, R_h and $\mu_2/\bar{\Gamma}^2$ were determined at 5.0 mM HTAC, the maximum HTAC concentration investigated in wall shear stress measurements. However, for PEO20, we also measured D_0, R_h and $\mu_2/\bar{\Gamma}^2$ at HTAC concentrations equal to 0.2 mM, i.e. near the MBC. In all cases, Table 2 shows that the hydrodynamic radius of PEO-HTAC complexes is observed to be largest in the absence of added salt. The addition of salt at a mole ratio of [NaCl]/[HTAC] = 1/1 decreases R_h, substantially, but a further increase of salt to a mole ratio of NaCl/HTAC = 5/1 results in a slight increase in R_h. Our results are consistent with the previous published data reported by Mya et al. [28], who compared R_h values at MBC for PEO-HTAC solutions in the absence of added salt and with 0.1 M KNO_3 added. Addition of 0.1 M KNO_3 was observed to reduce the value of R_h, due to the combined effects of polymer chain contraction via electrostatic screening and dissociation of multichain complexes. The reason for the small increase in R_h at higher salt is not clear, but may reflect an increase in the bound micellar radius, analogous to that observed in free micelles.

Finally, we comment on results for the normalized second cumulant, $\mu_2/\bar{\Gamma}^2$ which is a measure of the variance in the distribution of hydrodynamic radii. For HTAC and HTAC-NaCl with a mole ratio of 5, $\mu_2/\bar{\Gamma}^2$ values are 0.16 and 0.07,

respectively. For PEO6_40 + HTAC 5 mM and PEO6_40 + HTAC 5 mM + [NaCl]/[HTAC] = 5/1, $\mu_2/\bar{\Gamma}^2$ values are 0.83 and 0.23, respectively. For PEO20_15 + HTAC 0.2 mM and PEO20_15 + HTAC 0.2 mM + [NaCl]/[HTAC] = 5/1, $\mu_2/\bar{\Gamma}^2$ values are 0.45 and 0.34, respectively. These results are consistent with the previous results of Mya et al. [28]. They investigated the particle size distribution (PSD) of PEO-HTAC in the solution with and without KNO_3 and found that PEO-HTAC in salt solution showed a narrow size distribution comparing to PEO-HTAC in the free-salt solution. Our results indicate that addition of salt reduces the size polydispersity of the micelles and polymer–surfactant complexes.

3.3. Wall shear stress measurements

Fig. 5 exhibits the variation of wall shear stress, τ_w, at $Re = 5000$, as HTAC concentration is increased for HTAC solutions at 30 °C, without salt, and with salt added at mole ratios [NaCl]/[HTAC] equal to 1.0 and 5.0. For salt-free HTAC, the wall shear stress decreases with increasing concentration up to an optimum concentration, $c^*_{HTAC} = 1.7$ mM, where we find a maximum drag reduction of about 51%. Above c^*_{HTAC}, the wall shear stress shows a slight increase with HTAC concentration. With salt added at NaCl/HTAC mole ratios of 1.0 and 5.0, the wall shear stresses of these solutions initially decreases as the salt-free solution, but exhibits minima at optimum concentrations, c^*_{HTAC}, ≈0.9 and 0.3 mM, respectively, which are much larger than the salt-free case, after which a sharp rise to a constant value is seen. The corresponding maximum drag reductions are 56% and 39%, respectively. Here, we note that the CMC of HTAC in aqueous HTAC, [NaCl]/[HTAC] = 1/1 and [NaCl]/[HTAC] = 5/1 solutions occurs at approximately 1.3, 0.7 and 0.6 mM; respectively. These values are numerically comparable to the respective optimum HTAC concentrations of those solutions, so we observe significant an apparent drag reduction prior to micelle formation. This is an unexpected result, and its origin is presently unclear which may be related to lowering of the surface tension. Another possibility is that the CMC is somehow reduced in the turbulent flow field. Recent work [31] suggests that the mixed shear and extensional character of such flows may promote micelle formation leading to local concentrations of surfactant that are much larger than the mean value. Another possibility is that individual surfactant molecules and/or micelles migrate preferentially towards the walls to reside in the viscous sublayer causing the wall slip.

In micelle-driven drag reduction, the optimum HTAC concentration decreases with ionic strength, because the micellar size increases with ionic strength, due to neutralization of electrostatic repulsions between surfactant head groups [32–34]. We further observe in Fig. 5 an increase in wall shear stress or a diminished drag reduction in the presence of added salt at HTAC concentrations beyond the CMC. We attribute this to the increased viscous resistance because of the presence of increasing numbers of micelles.

Fig. 6 shows the dependence of wall shear stress, τ_w, on HTAC concentration at $Re = 5000$ and at 30 °C for PEO6_40 + HTAC, PEO6_40 + [NaCl]/[HTAC] = 1/1 and PEO6_40 + [NaCl]/[HTAC] = 5/1, respectively. Here, we find that wall shear stress of PEO6_40 + HTAC monotonically increases with increasing HTAC concentration to an essentially constant value as the HTAC concentration approaches the CMC ($CMC_{PEO6\_40+HTAC} = 1.70$ mM). Likewise, the wall shear stresses of PEO6_40 + [NaCl]/[HTAC] = 1/1 and PEO6_40 + [NaCl]/[HTAC] = 5/1 increase with HTAC concentration to a maximum value near their respective CMCs ($CMC_{PEO6\_40+[NaCl]/[HTAC]=1/1} = 1.50$ mM and $CMC_{PEO6\_40+[NaCl]/[HTAC]=5/1} = 1.00$ mM), after which, the wall shear stresses decrease to smaller asymptotic values at HTAC concentrations in excess of 4.0 mM. At HTAC concentration of 5.0 mM, the percentage of drag reduction are 4%, 64% and 84% for the aqueous solutions of PEO6_40 + HTAC, PEO6_40 + [NaCl]/[HTAC] = 1.0 and PEO6_40 + [NaCl]/[HTAC] = 5.0, respectively. Recalling that the PEO concentration was fixed at the optimum concentration

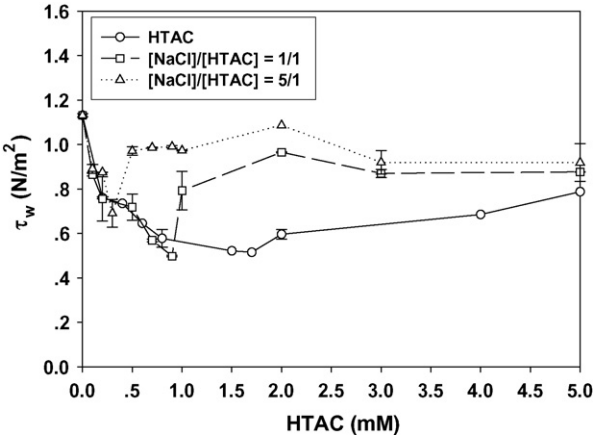

Fig. 5. Dependence of wall shear stress, τ_w, on HTAC concentration of aqueous HTAC solutions with and without NaCl added at 30 °C, $Re = 5000$: (a) HTAC; (b) [NaCl]/[HTAC] = 1/1, the mole ratio of NaCl to HTAC equal to 1; and (c) [NaCl]/[HTAC] = 5/1, the mole ratio of NaCl to HTAC equal to 5.

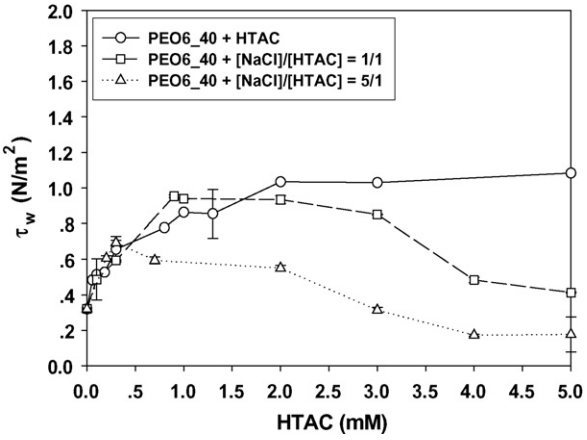

Fig. 6. Dependence of wall shear stress, τ_w, on HTAC concentration for aqueous PEO6_40 + HTAC solutions with and without NaCl added at 30 °C, $Re = 5000$: (a) PEO6_40 + HTAC, PEO M_w 6.06×10^5 g/mol at 40 ppm; (b) PEO6_40 + [NaCl]/[HTAC] = 1/1, PEO M_w 6.06×10^5 g/mol, 40 ppm, and the mole ratio of NaCl to HTAC equal to 1; and (c) [NaCl]/[HTAC] = 5/1, PEO M_w 6.06×10^5 g/mol, 40 ppm, and the mole ratio of NaCl to HTAC equal to 5.

for drag reduction in the absence of surfactant (c^*_{PEO}), the observed increase in wall stress on titration with HTAC was demonstrated in our earlier work [22] to arise because the presence of HTAC causes a shift in c^*_{PEO} from 40 mM to lower PEO concentration. Fig. 6 further shows that the increase in the wall stress occurs at very low added levels of HTAC, below the nominal CAC and MBC values (Table 1). As noted and confirmed in our earlier study [22], this implies that the CAC and MBC are presumably reduced in turbulent flow, which allows a shift of the optimum HTAC concentration, $c^*_{HTAC\text{-}PEO}$ to a lower value. A third feature of Fig. 6 is that, when the HTAC concentration is above the MBC, increase in the NaCl/HTAC mole ratio produces a decrease in wall shear stress. This effect may be related to the more stabilized PEO-HTAC complex formation and possibly to the reduction in the PEO chain rigidity resulting from the dissociation of multichain complexes (see Fig. 9). Our result is opposite to the generally accepted idea that turbulent wall shear stress decreases with increasing hydrodynamic volume.

In Fig. 7, we exhibit the variation in wall stress, τ_w, with HTAC concentration at $Re = 5000$ and 30 °C, for PEO-HTAC solutions containing high-molecular weight PEO, viz. PEO20_15 + HTAC, PEO20_15 + [NaCl]/[HTAC] = 1/1 and PEO20_15 + [NaCl]/[HTAC] = 5/1. The data displayed in Fig. 7 show essentially the identical behavior to that seen in Fig. 6 for lower molecular weight PEO. At high concentrations of HTAC, beyond the CMC, τ_w is lowered in the presence of NaCl. The percentage of drag reduction when HTAC concentration reach to 5.0 mM are 0%, 27% and 39% for the aqueous solutions of PEO20_15 + HTAC, PEO20_15 + [NaCl]/[HTAC] = 1.0 and PEO20_15 + [NaCl]/[HTAC] = 5.0, respectively. An additional feature manifested in Fig. 7 is that the initial rate of increase of τ_w on titration with HTAC is clearly slower in the presence of added salt. This suggests that the presence of salt results in a smaller shift of the optimum concentration for drag reduction.

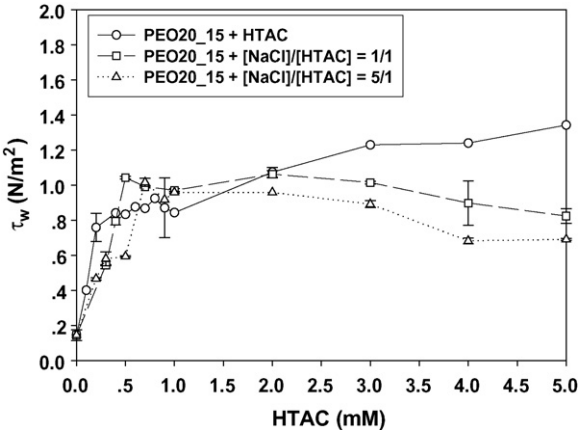

Fig. 7. Dependence of wall shear stress, τ_w, on HTAC concentration for aqueous PEO20_15 + HTAC solutions with and without NaCl added at 30 °C, $Re = 5000$: (a) PEO20_15 + HTAC, PEO M_w 17.9×10^5 g/mol, 15 ppm; (b) PEO20_15 + [NaCl]/[HTAC] = 1/1, PEO M_w 17.9×10^5 g/mol, 15 ppm, and the mole ratio of NaCl to HTAC equal to 1; and (c) [NaCl]/[HTAC] = 5/1, PEO M_w 17.9×10^5 g/mol, 15 ppm, and the mole ratio of NaCl to HTAC equal to 5.

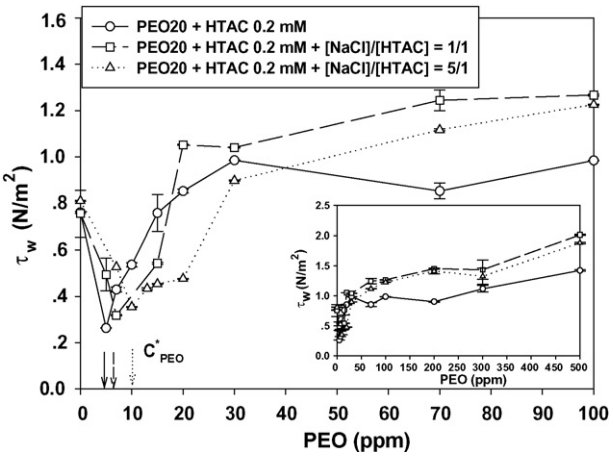

Fig. 8. Dependence of wall shear stress, τ_w, on HTAC concentration for aqueous PEO20 + HTAC at MBC; PEO M_w 17.9×10^5 g/mol and HTAC = 0.2 mM solutions with and without NaCl added at 30 °C, $Re = 5000$: (a) PEO20 + HTAC 0.2 mM; (b) PEO20 + HTAC 0.2 mM + [NaCl]/[HTAC] = 1/1, the mole ratio of NaCl to HTAC equal to 1; and (c) PEO20 + HTAC 0.2 mM + [NaCl]/[HTAC] = 5/1, the mole ratio of NaCl to HTAC equal to 5.

To confirm this, as shown in Fig. 8, the dependence of wall shear stress on PEO concentration was examined at $Re = 5000$ and 30 °C for PEO20 in aqueous solution containing 0.20 mM HTAC (corresponding to the MBC of 15 ppm PEO20), without salt and with salt added at mole ratios [NaCl]/[HTAC] = 1/1 and 5/1. Fig. 8 indicates that, indeed, the optimum PEO concentration for maximum drag reduction increases with addition of salt, having values $c^*_{PEO/HTAC} = 5$, 7 and 10 ppm, at which the maximum DR values are 77%, 72% and 69%, for solutions with [NaCl]/[HTAC] = 0, 1.0 and 5.0, respectively. At low PEO concentration, $c_{PEO} < 30$ ppm, the increase in the optimum PEO concentration and the increase in the wall shear stress with salt addition correlate approximately with the decreased hydrodynamic volume of the PEO-HTAC complexes due to the effects of polymer chain contraction via the electrostatic screening and the dissociation of multichain complexes (Table 2). At high PEO concentration, $c_{PEO} > 30$ ppm, the wall shear stresses of PEO-HTAC complex in salt solution are higher than that in water, with the wall shear stress of the solution having [NaCl]/[HTAC] = 1.0 being slightly greater than that of [NaCl]/[HTAC] = 5.0. The wall stress in this region may have derived from the increased solution viscosity when salt is added. Noting that in this case, as PEO concentration increases, the surfactant content falls increasingly below the MBC level, perhaps the hydrodynamic volume of PEO is increased in the presence of salt for surfactant depleted complexes.

Fig. 9a and b illustrates schematic drawings of complexes formed in PEO + HTAC in the absence and in the presence of NaSal in aqueous solution, respectively, when HTAC concentration is above CMC. In the salt-free aqueous solution, binding of micelles on multichain polymer–surfactant complexes occurs in the solution, and electrostatic repulsions lead to an increase in hydrodynamic volume of polymer–surfactant complex [27]. In the presence of salt, the number of bound HTAC molecules per chain increases substantially, i.e. the added salt stabilizes the binding of HTAC micelles to the polymer and single chain

(a) PEO + HTAC (b) PEO + HTAC + NaCl

Fig. 9. Schematic drawings of PEO and HTAC in aqueous solution without salt and in the presence of salt when HTAC concentration is above CMC: (a) PEO + HTAC and (b) PEO + HTAC + NaCl. ⊕ is cationic surfactant head group; ∼ is surfactant tail group; − negative counterion; ↔ repulsive force between surfactant head group; ∩ long chain PEO.

complexes are predominantly formed [28]. In addition, the hydrodynamic volume of PEO-HTAC complex in the presence of salt is reduced due to effects of polymer chain contraction via the electrostatic screening and the dissociation of multichain complexes.

4. Conclusions

We investigated the influence of ionic strength on CAC, CMC, MBC and hydrodynamic radius in aqueous solutions of HTAC and PEO-HTAC mixtures at 30 °C. Consistent with literature results, the values of CAC and CMC from conductivity and surface tension measurements indicate that salt stabilizes micelle formation in HTAC solutions and, in PEO-HTAC solutions, enhances the binding of HTAC micelles to the polymer. We also observe an increase in hydrodynamic radius of HTAC micelles at the MBC of HTAC in the presence of added salt and a decrease in R_h for the PEO-HTAC complexes in salt solution. These observations can be described, on the one hand to screening of electrostatic repulsions between surfactant head groups on HTAC micelles, and on the other, to PEO chain contraction via electrostatic screening and dissociation of multichain PEO-HTAC complexes. Wall shear stress measurements on HTAC solutions reveal that the optimal concentration for maximum drag reduction decreases with increasing molar ratios of NaCl to HTAC. The possible mechanisms of drag reduction in these solutions may be a surface tension effect, the decrease in the number of free micelles in aqueous HTAC solution, the decrease in the CMC in the turbulent flow field, or several effects combined. In PEO solutions on titration with HTAC, the wall stress increases up to the CMC and then decreases or levels off. This is due to a shift of the optimum concentration for drag reduction to a smaller value, the magnitude of the shift decreasing with increase of ionic strength.

Acknowledgements

S. Suksamranchit would like to acknowledge the financial support from the Thailand Research Fund (TRF), the RGJ grant no. PHD/0149/2543. This work was financially supported by the fund from MTEC, grant no. MT-43-POL-09-144-G, and the funds from the ADB Consortium Grant, and the Conductive and Electroactive Polymer Research Unit of Chulalongkorn University.

References

[1] P.S. Virk, H. Baher, Chem. Eng. Sci. 25 (1970) 1183.
[2] G.D. Rose, K.L. Foster, J. Non-Newtonian Fluid Mech. 31 (1989) 59.
[3] N.S. Berman, Ann. Rev. Fluid Mech. 10 (1978) 47.
[4] B.A. Toms, Proceedings of the First International Congress of Rheology, vol. 2, North-Holland, Amsterdam, 1949, p. 135 (Section II).
[5] J. Golda, Chem. Eng. Commun. 43 (1986) 53.
[6] R.P. Singh, in: N.P. Chermisinoff (Ed.), Encyclopedia of Fluid Mechanics, vol. 9, Gulf Publishing, Houston, 1990 (Chapter 14).
[7] R.A. Mostardi, L.C. Thomas, H.L. Green, F. VanEssen, R.F. Nokes, Biorheology 15 (1978) 1.
[8] A.G. Fabula, Trans. ASME J. Basic Eng. 93D (1971) 453.
[9] H.L. Greene, R.F. Mostardi, R.F. Wokes, Polym. Eng. Sci. 20 (1980) 499.
[10] J.G. Oldroyd, Proceedings of the First International Congress on Rheology, vol. II, North Holland, Amsterdam, 1948, p. 180.
[11] J.L. Lumley, Ann. Rev. Fluid Mech. 1 (1969) 367.
[12] J.L. Lumley, J. Polym. Sci., Macromol. Rev. 7 (1973) 263.
[13] J.L. Lumley, Phys. Fluids 20 (10) (1997) S64–S71 (Pt II).
[14] P.S. Virk, AIChE J. 21 (1975) 625.
[15] B. Hlavacek, L.A. Rollin, H.P. Schreiber, Polymer 17 (1976) 81.
[16] P.G. De Gennes, Physica 140A (1986) 9.
[17] P.G. De Gennes, in: A. Luigi (Ed.), Introduction to Polymer Dynamics: An Elastic Theory of Drag Reduction, Cambridge University Press, Cambridge, Great Britain, 1990 (Chapter 4).
[18] G. Ryskin, Phys. Rev. Lett. 59 (18) (1987) 2059.
[19] H.J. Choi, M.S. Jhon, Ind. Eng. Chem. Res. 35 (1996) 2993.
[20] J.L. Zakin, B. Lu, H.W. Bewersdorff, Rev. Chem. Eng. 14 (1998) 253.
[21] R.W. Paterson, F.H. Abernathy, J. Fluid Mech. 43 (1970) 689.
[22] S. Suksamranchit, A. Sirivat, A.M. Jamieson, J. Colloid Interface Sci. 294 (2006) 212.
[23] J. Myska, Z. Lin, P. Stepanek, J.L. Zakin, J. Non-Newtonian Fluid Mech. 97 (2001) 251.
[24] J. Myska, Z. Chara, Exp. Fluids 30 (2) (2001) 229.
[25] O. Anthony, R. Zana, Langmuir 10 (1994) 4048.
[26] K.Y. Mya, A. Sirivat, A.M. Jamieson, Langmuir 16 (2000) 6131.
[27] K.Y. Mya, A. Sirivat, A.M. Jamieson, Macromolecules 34 (2001) 5260.
[28] K.Y. Mya, A. Sirivat, A.M. Jamieson, J. Phys. Chem. B 107 (2003) 5460.
[29] W. Brown, J. Fundin, M.D. Miguel, Macromolecules 26 (26) (1992) 7192.
[30] M.J. Schwuger, J. Colloid Interface Sci. 43 (1973) 491.
[31] K. Arora, R. Sureshkumar, M.P. Scheiner, J.L. Piper, Rheol. Acta 41 (2002) 25.
[32] W. Brown, J. Fundin, M.D. Miguel, Macromolecules 26 (26) (1992) 7192.
[33] J. Myska, P. Stepanek, J.L. Zakin, Colloid Polym. Sci. 275 (1997) 254.
[34] B. Lu, Y. Zheng, H.T. Davis, L.E. Scriven, Y. Talmon, L. Zakin, Rheol. Acta 37 (1998) 528.
[35] E.M. Sparrow, W.D. Munro, V.K. Jonsson, J. Fluid Mech. 20 (1964) 35.